


RESEARCH

Open Access



# Thermal Resistance of Insulated Precast Concrete Sandwich Panels

Sani Mohammed Bida<sup>2</sup>, Farah Nora Aznieta Abdul Aziz<sup>1\*</sup> , Mohd Saleh Jaafar<sup>1</sup>, Farzad Hejazi<sup>1</sup> and Nabilah Abu Bakar<sup>1</sup>

## Abstract

Many nations are already working toward full implementation of energy efficiency in buildings known as Green Building. In line with this perspective, this paper aims to develop a thermally efficient precast concrete sandwich panels (PCSP) for structural applications. Therefore, an experimental investigation was carried out to determine the thermal resistance of the proposed PCSP using Hotbox method and the results were validated using finite element method (FEM) in COMSOL Multiphysics Software. The PCSP were designed with staggered shear connectors to avoid thermal bridges between the successive layers. The staggered connectors are spaced at 200 mm, 300 mm and 400 mm on each concrete layer, while the control panel is designed with 200 mm direct shear connection. In the experimental test, four (4) panels of 500 mm × 500 mm and 150 mm thick were subjected to Hotbox Test to determine the thermal resistance. The result shows that thermal resistance of the PCSP with staggered shear connection increases with increase in spacing. The PCSP with 400 mm staggered shear connectors indicates the best thermal efficiency with a thermal resistance (*R* value) of 2.48 m<sup>2</sup>K/W. The thermal performance was verified by FEA which shows less than 5% error coupled with a precise prediction of surface temperature gradient. This indicates that, with conventional materials, thermal path approach can be used to develop a precast concrete building with better thermal resistant properties. Hopefully, stakeholders in the green building industry would find this proposed PCSP as an alternative energy efficient load bearing panel towards sustainable and greener buildings.

**Keywords:** Green buildings, Precast concrete, Sandwich panel, Shear connection, Staggered connection, Thermal resistance

## 1 Introduction

Global warming has become a worldwide issue due to its impact on the environmental temperature that subsequently cause discomfort in buildings (Graziani et al., 2017). Convective thermal irradiation from the external environment usually transfer into the buildings. This call for the need for additional energy to condition the building by heating/cooling (Pérez-Lombard et al., 2008). This assertion is in line with the report by Woltman et al.

(2017) who inferred that space cooling and heating due to environmental changes have called for a renewed attention in terms of thermal resistance of building envelopes. Similarly, Retzlaff (2009) emphasized on a renewed determination for energy efficiency and conservation in buildings due to the effect of global warming. A properly designed and energy efficient building components can save as much as 70% energy demand during the life cycle of buildings (Ahmad et al., 2014). This is because buildings are the major users of grid energy supply with a total electricity consumption of about 75% of energy generated (Menoufi et al., 2012). Therefore, the phenomenon of increasing energy demand in buildings has serious consequences on our environment and should be given careful attention.

\*Correspondence: farah@upm.edu.my

<sup>1</sup> Housing Research Centre (HRC), Department of Civil Engineering, Universiti Putra Malaysia (UPM), 43400 Serdang, Selangor, Malaysia  
Full list of author information is available at the end of the article  
Journal information: ISSN 1976-0485 / eISSN 2234-1315

In modern architecture, green and sustainable buildings are receiving global attention (Boafo et al., 2016). In this approach, heat exchange between the inner and outer parts of building is minimized (Graziani et al., 2017). The recent innovation that involved provision of insulation layers between building assemblies has attracted more attention to precast concrete components which led to the tremendous growth in thermally efficient and sustainable buildings. According to Al-Ajlan, (2006), energy conservation in buildings could be made more effective by providing insulation at its core. This assertion was supported by Hacker et al., (2008) who mentioned that annual energy requirement in household could be reduced by insulating the building components.

Many stakeholders and agencies of governments have key-in to the policy of sustainable and energy efficient building across the world. The European Union and US Department of Energy (DOE) have targeted year 2020 for new buildings to comply with their nearly zero energy building policy” (Sartori et al., 2012). In Malaysia, Green Building Index (GBI) was established in 2009 with a mandate to have a paradigm shift to a more sustainable green buildings and factories before the year 2020. More of these policies are gradually being proposed across governments and nations toward sustainable and energy efficiency in buildings. In Australia and Singapore, Green Star and Green Mark, respectively, have been established (Chua & Oh, 2011). Therefore, more sustainable approach that minimizes exchange of heat energy through the building assemblies with the aid of insulation material such as PCSP could be the future of green buildings. According to Gervásio et al. (2010), energy sustainability can only be achieved in buildings through the use of insulation material.

Many investigations have been carried out on precast concrete sandwich panels using different materials for shear connection and wythes. Precast concrete sandwich panels made from conventional steel and concrete materials have demonstrated sound structural integrity, but with low thermal efficiency and many unreported thermal performance (Bai & Davidson, 2015; Benayoune et al., 2008; Bush & Stine, 1994; Bush Jr & Wu, 1998; Carbonari et al., 2013; Hamed, 2016; Joseph et al., 2017; Lee & Pessiki, 2008). This has prompted the use of alternative

material with low thermal conductivity other than steel and usual concrete for wythes and shear connectors, respectively. Fibre reinforced polymer materials such as glass fibre, carbon fibre, basalt fibre etc. have attempted for use in PCSP toward achieving low thermal conductivity (Choi et al., 2015; Einea et al., 1991; Frazão et al., 2018; Hamed, 2017; Hodicky et al., 2014; Kim & You, 2015; Naito et al., 2011; Salmon et al., 1997; Teixeira et al., 2016; Tomlinson & Fam, 2016; Woltman et al., 2017; Zhi & Guo, 2017). However, these materials were reported to exhibit low shear strength, brittleness, de-bonding/bond-slip and high cost.

Also, foamed concrete is used for precast concrete sandwich panel wythe to reduce their density and thermal conductivity (Amran et al., 2015, 2018; Mohamad & Hassan, 2013; Mohamad & Muhammad, 2011; Mohamad et al., 2011). However, de-bonding crushing effect, longer shear connector embedment length and larger concrete section are necessary to ensure structural stability. According to Amran et al. (2015), thermal insulation of 0.04 W/mK is achieved in every 100 kg/m<sup>3</sup> density decrease of foam concrete. However, the decrease in density have significant negative consequences on the structural capacity of a panel made with the foamed concrete. Because, it increases porosity which leads to corresponding decrease in compressive strength of concrete. Therefore, such concretes with low compressive strength and high susceptibility to water absorption are not advisable to serve load bearing members.

Therefore, the main contribution of this paper is to develop a thermal resistant two layered PCSP using conventional materials through systematic control of the shear connectors contact between the two layers refers to as thermal path.

## 2 Experimental test

### 2.1 Material properties

Concrete of 40 MPa target strength produced for the PCSP wythes using mix composition shown in Table 1. The coarse aggregate of 10 mm maximum size was selected to allow good workability of concrete in the 40 mm thick panel. This is based on best practice of providing maximum aggregate size of not more than a quarter of the thickness of the specimen. Similarly, the mortar

**Table 1** Concrete mix proportion.

Concrete	Concrete materials (kg/m <sup>3</sup> )				W/C	SP (%)
	FA	CA	Cement	Water		
Wythes	680	1020	500	200	0.4	-
Stud	2846	-	1035	587	0.5	0.3

FA Fine aggregate, CA coarse aggregate, W/C water cement ratio, SP superplasticizer

of 40 MPa was designed to connect the two concrete wythes together and this portion is name as column stud. The compressive strength at 28 days is measured by 100 mm and 50 mm cubes for concrete and mortar specimens, respectively, in accordance to BS EN 206-1 (2000).

Mild steel wire mesh of 6 mm diameter spaced at 100 mm was used as reinforcement in the concrete layers, while for shear connection, the longitudinal reinforcement bars of 10 mm high strength and 250 MPa yield strength of the mild steel is 250 MPa was used. Polystyrene was used for the insulation between the two individual layers and glued with the aid of polystyrene friendly adhesives during panel assembly.

### 2.2 Specimen Details

The specimen size used for the thermal resistance test is taken from the full-scaled precast concrete sandwich panel (PCSP) shown in Fig. 1. The full-scaled panel is 3000 × 1650 × 150 mm in size, while the specimen size was estimated based on the width of column stud (150 mm) plus half the flange dimension from both sides of the column stud. The dimension was finally rounded up to 500 mm in conformity with the available equipment (Hotbox) in the laboratory. The difference between the samples in the staggered shear connection is the spacing at 200 mm, 300 mm and 400 mm on each side of the wythes and are designated as P2, P3 and P4, respectively. The connector spacing was limited to the maximum of 400 mm due to the maximum attainable height of 500 mm dimension of the specimen. Shear capacity of the connectors are improved through embedment of the

connectors in concrete stud. This approach increase load capacity and resistance to shear deformation of the panels as reported by Tomlinson and Fam (2014).

The sample details through the column stud is shown in Fig. 2 with the dimension and section thickness of 500 × 500 mm and 150 mm, respectively, as indicated in Fig. 1. Part of the concrete area between the studs are reduced by the insulation material. This systematically reduced the supposedly three PCSP layers to two which makes the panel more economical.

### 2.3 Specimen Preparation

The samples were produced using assembling process with each wythes of the panels being prepared independently. The preparation process involve three stages, namely; (i) formwork design and fabrication, (ii) concrete production and casting of the individual wythes, and (iii) the assembling of the independent wythes to form a complete panel.

The timber formworks were prepared by assembling the component parts together and the reinforcement wire mesh were placed in the formwork with about 50 mm clearance from all sides of the formwork. Alignment of the shear connectors was ensure with the aid of guard rail arranged above the formworks.

Concrete mix proportions specified in Table 1 was prepared and poured in a formwork placed on a vibrating table to ensure proper compaction during the casting operation. The top surface was levelled to ensure a levelled surface for subsequent bonding with polystyrene. The specimens were strip-off the formworks after 24 h and water cured for the period of 28 days.

The assembling operation was carried out by initially placing the polystyrene on the surface of each wythes (Fig. 3a) with the aid of polystyrene friendly adhesive. The two individual wythes were clamped together after the insulation process as shown in Fig. 3b and connected through the column stud using vertical twin shear reinforcement bars. The column studs were cast using mortar slurry to prevent segregation. Fig. 3c shows the completed panel ready for curing and subsequent testing.

### 2.4 Experimental Method

The thermal resistance tests were conducted with Hot Box test apparatus setup in the Housing Research Centre, Universiti Putra Malaysia (UPM). The experiment was conducted in consistent with the provision of ASTM C1363 (2019). Each face of the specimens is mounted with 5 Type K surface thermocouples; one on each of the four (4) corners of the specimens and additional one at the middle of the specimens for surface temperature measurements. Another two (2) heat flux sensors were attached on the same of the specimens to monitor the

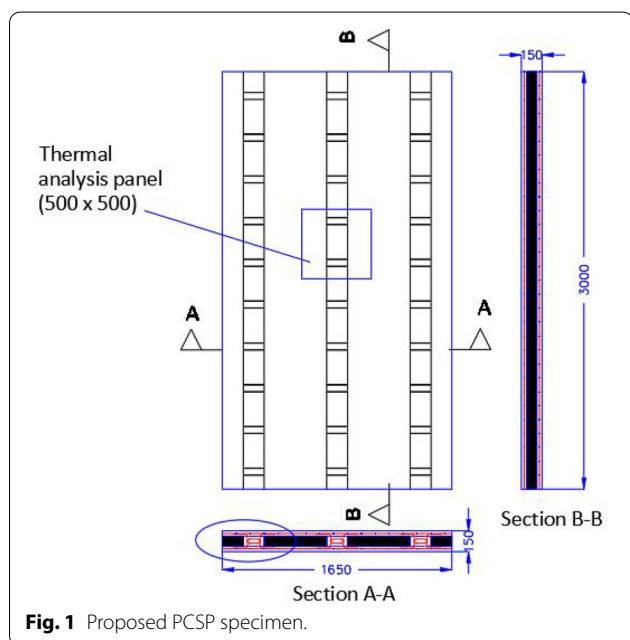
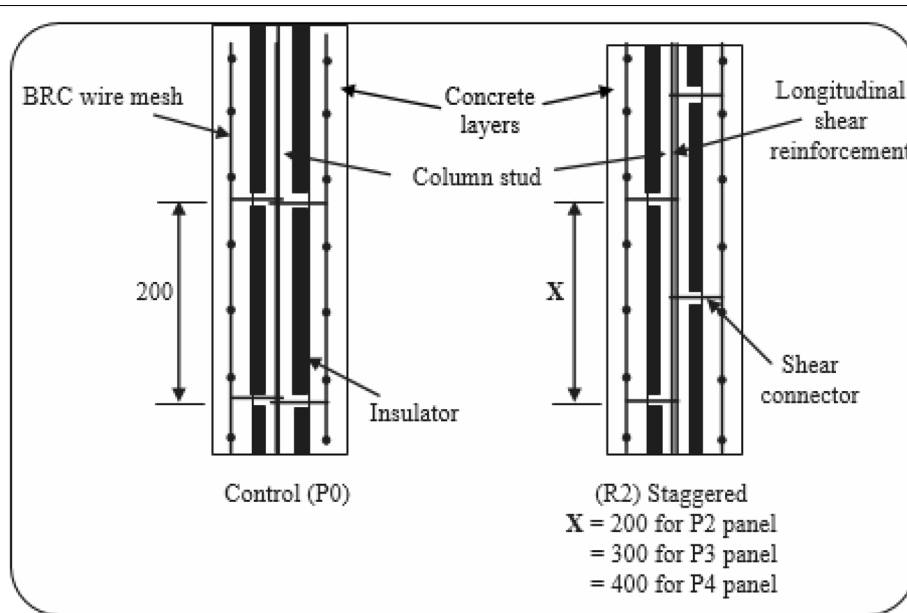


Fig. 1 Proposed PCSP specimen.



**Fig. 2** Section details through the column stud of the PCSP.



**Fig. 3** Construction process: **a** insulation, **b** assembling and **c** completed panel.



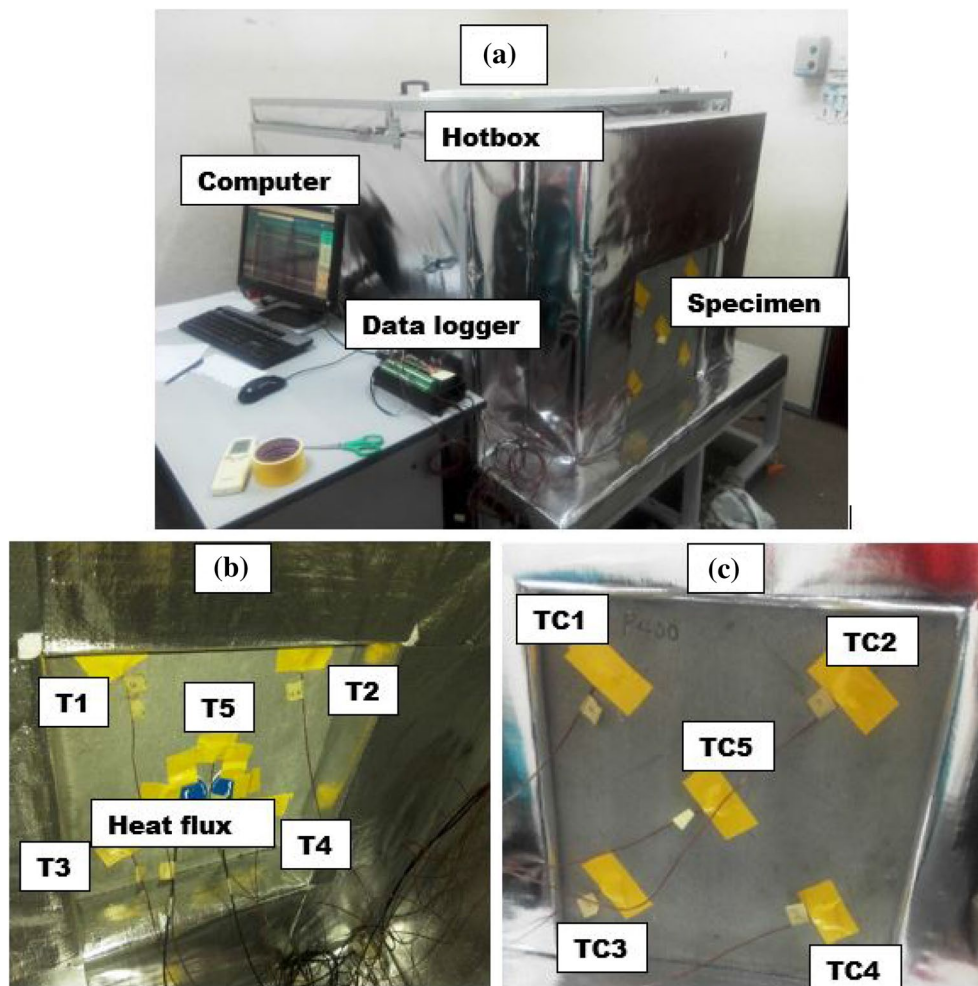


**Fig. 4** Experimental setup **a** Hotbox apparatus **b** hot and **c** cold surfaces of the specimen.

heat flow rate ( $Q$ ) of the specimens. Fig. 4 shows the sensors attached to the specimen surfaces. Apart from the specimen surfaces, one thermocouple is provided in each room to measure the air temperature during the test. In addition, an anemometer and hygrometer were used to measure the wind speed and humidity in the Hotbox test machine. All the devices are attached to the surface of the samples on one end with the aid of adhesive tape and to the data logger on the other end.

The Hot Bot machine comprise a window  $500 \times 500$  mm, where the specimens are mounted one at a time as shown in Fig. 4a. The ambient surface of the specimen faces the inner part of the Hot Box machine and is called the hot face (H), while the other surface faces the air conditioned room and is called the cold face (C). The devices were setup on a computer controlled machine connected to the data logger to monitor the readings. The devices were configured based on the factory default parameters provided by the manufacturers

before commencement of the experiment. Continuous data acquisition was ensured during the experiment for a period of 25 h with record taken every minute until the end of each experiment when steady state is attained.

### 3 Numerical Model

Besides Experimental work, the thermal resistance properties were verified using Finite Element Analysis (FEM) model with the aid of COMSOL Multiphysics software (CM). This software is simulation environment that is highly interactive and consist of all the processes involved in modelling operation. The software is capable of simulating processes, devices and designs in most field of endeavours, such as building, scientific, manufacturing and engineering research (Al-Abidi et al., 2013; Gerlich et al., 2013; Royon et al., 2013; Van Schijndel et al., 2009).

The FEM simulation was carried out in a three-dimensional time-dependent heat convection module over 25 h

**Table 2** FEM material properties.

Materials	HC (J/kg K)	TC (W/m K)	References
Polystyrene	1300	0.037	(Gerlich et al., 2013)
Concrete	750	1.88	(Kontoleon et al., 2013)
Reinforcement	460	60	(Kim & You, 2015)

HC Heat capacity (J/kg K), TC Thermal conductivity (W/m K)

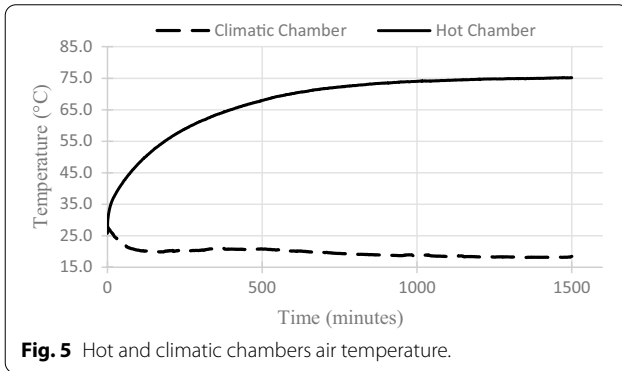


**Fig. 5** Hot and climatic chambers air temperature.

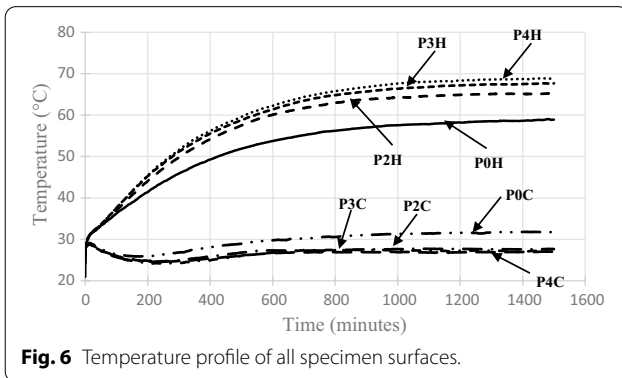


**Fig. 6** Temperature profile of all specimen surfaces.

period to imitate the conditions set up in the Hot Box experiment. Heat transfer analysis was simulated from ambient to cold surface through the specimen at a temperatures of 75 °C and 19 °C, respectively, as boundary conditions in line with the experimental setup. All other boundary conditions not assigned are by default full insulation unless redefined.

Heat transfer in solids was modelled with simultaneous airflow and heat transfer in the domain computed with Equations. (1)–(3) with heat generation incorporated into the energy conservation equation as follows:

$$q = -T\nabla \tag{1}$$

$$\rho C_p \frac{\partial T}{\partial t} + \rho C_p u \cdot T\nabla + \nabla \cdot q = Q_1 + Q_{red} \tag{2}$$

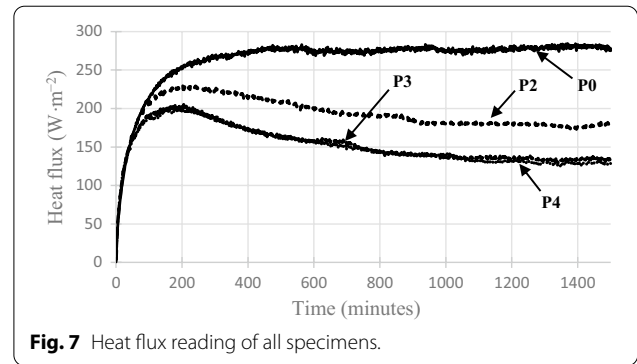


**Fig. 7** Heat flux reading of all specimens.

$$R = \frac{(T_1 - T_2)}{q} \tag{3}$$

where  $q$  is the heat flux,  $T_0$ ,  $T_1$  and  $\nabla T$  represent room, ambient and temperature difference, respectively, of the material at a particular location.  $\rho$  represents material density ( $\text{kg/m}^3$ ),  $C_p$  air specific heat capacity ( $\text{J kg}^{-1} \text{K}^{-1}$ ),  $u$  denotes the velocity field ( $\text{ms}^{-1}$ ),  $Q_{red}$  as the heat generation ( $\text{Wm}^{-3}$ ) and  $Q_1$  as heat loss ( $\text{Wm}^{-3}$ ). This equation is considered when transverse heat flows are neglected and only one-dimensional heat propagation was considered, provided there is no heat generated within the thermal mass of the panel.

Four sets of verification cases were simulated in the software in other to attain the steady state. The verification results achieved were analysed in relation to the experimental to ascertain the correlation level of the outcomes. The panels used as specimens in the actual hot-box experiment are similar to the FEA validation models. Table 2 shows the material properties used in the simulation at initial temperature of 26°.

## 4 Results and Discussion

### 4.1 Experimental Results

Fig. 5 shows the result of the hot box test which indicates that a steady state condition of 19–20 °C was attained at about 600–1000 min in the climate chamber, while in the hot chamber, a temperature in the range of 70–75 °C was attained. Therefore, based on the recommendation of ASTM C1363 (2019), the two temperatures ranges for the cold and hot chambers fall within the stipulated environmental conditions (– 40 to 85 °C).

Fig. 6 shows the results of the average ambient and cold specimen surface temperature achieved in all the specimens. The profiles P0H, P2H, P3H, and P4H are the temperature profiles for the hot or ambient surfaces, while P0C, P2C, P3C and P4C represent the temperature profile for the cold surfaces of the control panel, staggered panels spaced at 200, 300 and 400 mm,

respectively. The control sample (P0) indicated the least temperature differences between its ambient and cold faces. This indicates that huge amount of heat transfer took place across the specimen. The heat transmission could be associated with the direct shear connection in the specimen which proved that thermal bridges aids rapid heat transfer a panel system. In contrast, panel P4 shows the largest temperature different which decreases with reduction in shear connection spacing down to panel P2. The large temperature difference recorded in the staggered panels is due to the delay in the heat transmission across the panel as a result of the increase in the thermal path length. Since the two faces are at different temperature, the agitated molecules would vibrate across their lattices from hot region to cold region in other to attain equilibrium. The longer the spacing of the connectors the higher the distance required for each molecule to traverse to reach equilibrium position. This explain why heat transfer is directly proportional to the shear to the distance between the connectors' spacing. More, heat transfer parallel to the ambient surface ensured in the staggered connectors further delays heat transmission (ASHRAE Handbook, 2009).

Fig. 7 shows the heat flux results for the experiment test carried out over 25 h period for all the specimens. It is an indication of the quantity of heat transferred per unit area ( $W/m^2$ ). In this results, specimen P0 indicated the largest quantity of heat flows through, while the least was achieved in panel P4. This results is consistent with the temperature profile behavior recorded in Fig. 6. That is, the sample P0 which recorded the highest temperature on the cold face at the end of the experiment also shows the largest heat flux value. This shows that more heat energy is absorb through the specimen which is an indication of higher thermal transfer. More so, a perpetual heat transfer was observed in the control panel P0 after 400 min. However, other panels with staggered shear connections recorded lower heat transfer values at the same 400 min into the experiment. Therefore, this confirm that the thermal bridge in the control panel is the major cause of heat energy transfer. Conversely, the mechanism of heat energy transfer in the panels with staggered panels avoids thermal bridges which causes delay in the transmission process at the insulation layer, thus, the heat transfer at the end of the experiment (1500 min) is less. The process led to the heat flux results achieved of  $174 W/m^2$ ,  $128 W/m^2$  and  $127 W/m^2$  for the staggered panels P2, P3 and P4, respectively, compared with the highest value recorded for control P0 ( $276 W/m^2$ ). Since heat flux is the amount of heat energy that pass through a body.

**Table 3** Thermal resistance of the specimens.

Panel ID	Thermal resistance ( $m^2K/W$ )
P0	1.09
P2	1.73
P3	2.43
P4	2.48

This means that more energy has passed through the control panel as indicated by the higher flux value and decrease down to panel P4. This can be associated with the shorter travel distance for the agitated molecules in the panels. The thermal resistance recorded above is due to the insulation incorporated in the system and the thermal path applied in this research. Conclusively, it can be inferred that increase in travel distance leads to decrease in the degree of thermal (heat) transmission. However, no significant changes in heat transfer takes place between 300 to 400 mm staggered shear connector spacing.

Using the Guarded hot box test, Lee and Pessiki (2006) recommended the thermal resistance,  $R$  as.

$$R = \frac{A(T_1 - T_2)}{Q} \text{ in } m^2K/W \quad (2.1)$$

where  $A$  is unit area of a specimen ( $m^2$ );  $T_1$  and  $T_2$  are the area weighted mean temperatures of the two surfaces and  $Q$  ( $W$ ) is the heat flow through the panel under steady state conditions.

The average result obtained above as shown in Figs. 4, 5, 6 are incorporated in Eq. (2.1) to obtain the thermal resistance presented in Table 3. The computed result shows that the control specimen (P0) that exhibits direct thermal bridge attained the lowest thermal resistance of  $1.09 m^2K/W$ . The panels with staggered shear connections (P2, P3 and P4) showed improvement in thermal resistance recording  $1.73 m^2K/W$ ,  $2.43 m^2K/W$  and  $2.48 m^2K/W$ , respectively. Thermal resistance refers to the insulation capability of a system or body. This indicate that higher resistance represent higher insulation ability. The above result indicates an improvement in terms of insulation ability of about 58.7%, 122.9% and 127.5% for P1, P2 and P3 compared with the control P0. This result was achieved at a staggered difference in shear connector spacing of 100 mm each. The result further showed that, up to P3 significant thermal performance was achieved, but, P4 yield a minimal improvement in thermal resistance of about 5% compared with the P3. In this result, an economical panel sections are achieved with improved

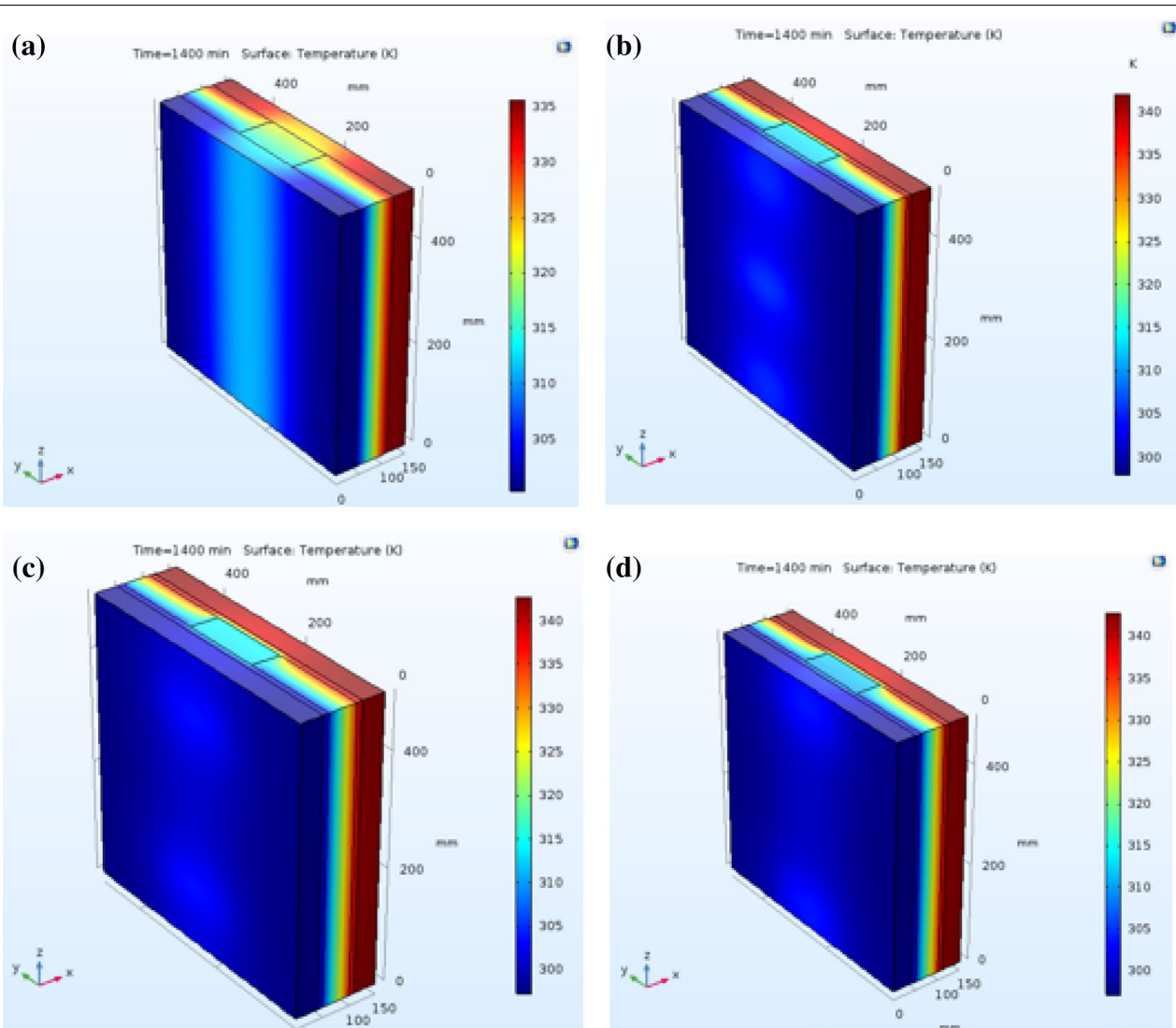


**Fig. 8** Simulated temperature gradient of panels **a** P0, **b** P2 **c** P3 and **d** P4.

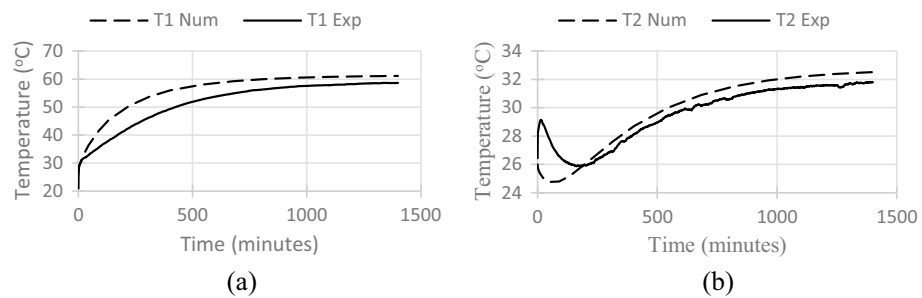


**Fig. 9** Experimental and numerical temperature profiles for the control panel (P0), **a** cold and **b** hot surfaces.



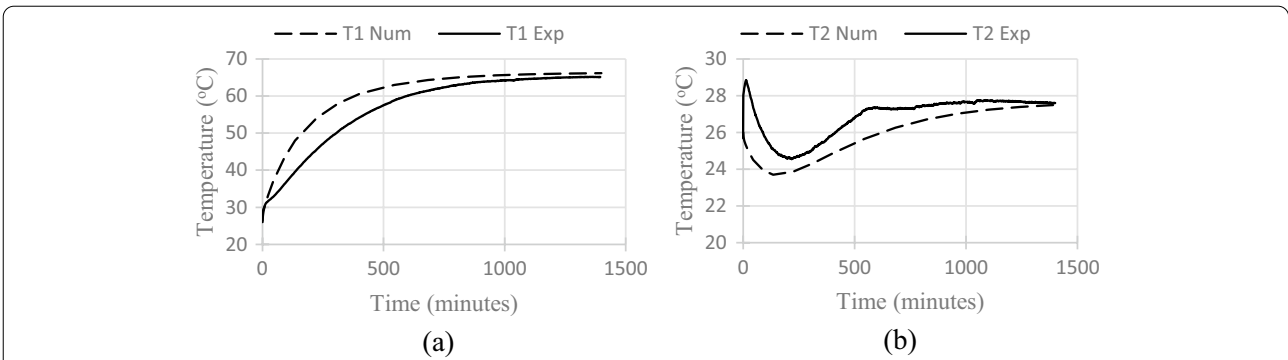


**Fig. 10** Experimental and numerical temperature profiles for panel P2, **a** cold and **b** hot surfaces.

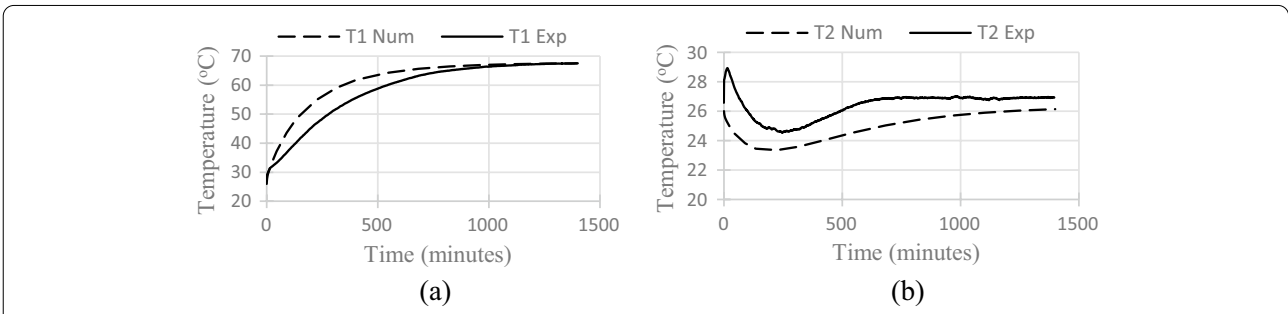


**Fig. 11** Experimental and numerical temperature profiles for panel P3 **a** cold and **b** hot surfaces.

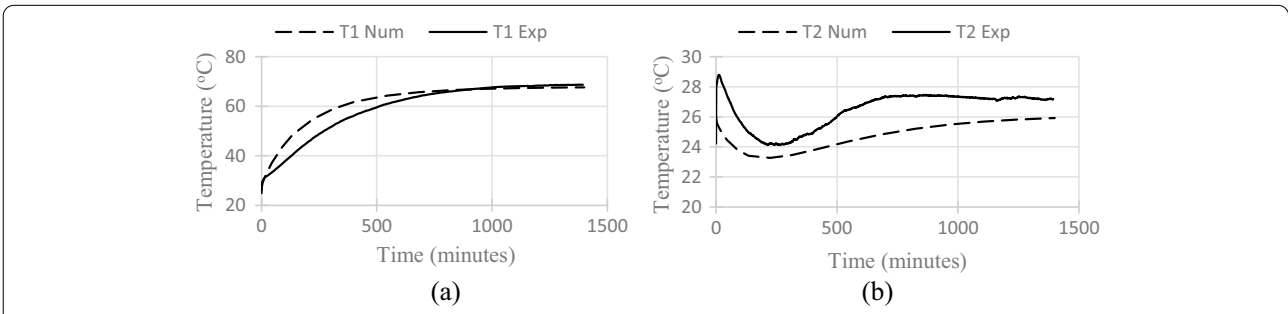


**Fig. 12** Experimental and numerical temperature profiles for the panel P4 **a** cold and **b** hot surfaces.

thermal resistance compared with the conventional solid panels.

**4.2 Numerical Results and Discussions**

The numerical analysis was undertaken to verify the thermal performance achieved in the experimental work of the PCSP using 3D finite element (FEA) model (COMSOL Multiphysics software). The result are presented in terms of temperature gradient of the specimens across the column stud as presented in Fig. 8. The rainbow

spectrum was used to represent the temperature gradient on the computer-generated model. The rainbow colour range Blue to Red colour represents increasing temperature from cool to the hottest surface. Fig. 8 shows that the intensity of the lighter blue at the area of column stud on the cold face reduces as the spacing of shear connection increases. This is consistent with the heat flux results which also reduces with increase in shear connection spacing. In addition, it is consistent with the experimental result shown in Fig. 6 which shows decrease in surface temperature with increase in shear connector spacing.

**Table 4** Verification of specimen temperature results.

Specimen	Ambient Surface Temperature (°C)			Cold face Temperature (°C)		
	Exp	FEM	Error (%)	Exp	FEM	Error (%)
P0	59.00	61.07	3.5	31.80	32.51	2.2
P2	65.15	66.14	1.5	27.60	27.50	0.4
P3	67.45	67.45	0.0	26.96	26.13	3.1
P4	68.69	67.70	1.4	27.16	25.92	4.6

Exp experimental, FEM finite element model

The dark blue and red colours on the cold and ambient faces are an indication of improved resistance to heat transfer achieved as a result of the full insulation on both sides of the column stud. In addition, it indicates that there exist variation in temperature from one location to the other on the specimen surface. The resistance achieved by the polystyrene at the column stud area is indicated by the similar colour indicated on the ambient surface (red). The control (P0) shows heat transfer from ambient side of the panel migrating through the column stud without obstruction.

#### 4.3 Validation of Results

Figs. 9, 10, 11, 12 show the experimental and simulated results carried out for verification purpose. The results comprise of ambient and cold surface temperature of the samples T1 and T2, respectively, conducted over 1400 min. The ambient temperature profiles are designated  $Num\_T_1$  and  $Exp\_T_1$  for the numerical and experimental results, respectively, while the cold surface temperature profiles are, respectively,  $Num\_T_2$  and  $Exp\_T_2$ .

The numerical and experimental results of the control sample (P0) is shown in Fig. 9a, b. Similar variation temperature profile is observed in both experimental and the numerical results. In both cases, steady state temperature was achieved at about 800 min to 1000 min in to the experiment. The numerical and experimental temperature recorded at steady state are 61.1 °C and 59 °C, respectively. The control specimen shows cold face temperature profile similar to the experimental curve. Although, between 0 to 20 min in to the experimental, a sudden change in temperature was recorded. Thereafter, the curve begins to conform to the values attained in the numerical result. Though, the case is not the same at the initial stage of the numerical analysis result. This phenomenon can be attributed to the cooling effect of the air conditioner stationed in the cold room. The initial cooling by the conditioner forces the air temperature downwards which is the effect recorded in the experimental that gradually stabilised. However, in the numerical model, a perfect condition is assumed

and a steady reduction of the temperature is ensured. This makes the curve to achieve a near perfect curve. Although, very close temperature values of 32.5 °C and 31.8 °C were achieved at steady state for the numerical and experimental results, respectively.

In the other hand, the experimental and numerical specimen temperature results of the P2, P3 and P4 with the staggered shear connectors are shown in Figs. 10, 11, 12. Both the experimental and numerical results behave in a similar manner until the experiments reached a steady state condition at 800–1000 min for cold surfaces and 600–800 min for the hot surface. An abrupt change in temperature was also observed at the beginning of the experiments (0 to 18 min) similar to the control specimen results. The sudden change in the temperature profile is attributed to the force convection of the air conditioner at the beginning of the experiment before the room becomes uniformly conditioned.

Table 4 shows the statistical analysis of the output values of both the numerical and experimental results. The FEM has predicted the heat transfer behavior of sandwich panels with high precision. Very good agreement was achieved between the experimental and the finite-element results. The results recorded 0–3.5% and 0.4–4.6% error for the ambient and cold surfaces, respectively. The higher error in the cold surface could be attributed to the sudden rise in temperature profile at the beginning of the experimental results as discussed earlier.

#### 5 Conclusions

Thermal resistance of precast concrete sandwich panels were experimentally assessed under steady-state condition using Hot Box method. Thus, the following conclusions are drawn.

1. The results achieved shows that thermal resistance of a panel is directly proportional to the length of the thermal path. It also indicated that staggering of shear connectors increases thermal path length and subsequently improve thermal resistance of panels.

2. Thermal path approach applied to panels made from conventional concrete and steel materials could offer improved thermal resistance without necessarily using alternative materials. In addition, the direction of thermal path, either perpendicular or parallel to the heat flow direction determines the time lag expected during the heat transfer process. Better thermal resistance is achieved with this method compared with the conventional shear connection methods.
3. A promising thermal resistance result was achieved of 2.48 m<sup>2</sup>K/W for sandwich panels with staggered shear connection.
4. The numerical analysis provided reliable output and save computation time and cost of having produce full-scaled panels. The numerical analysis was able to provided pictorial view of temperature contours of the specimen samples with less than 5% error rate.

#### Acknowledgements

The authors wish to acknowledge the contribution of Ministry of Science and Technology Malaysia (MOSTI) for providing the research grant (06-01-04-SF2364) used to carry out this research. We also thank other individuals such as technicians who contributed immensely in making this research a reality.

#### Authors' contributions

SM performed all the experimental works, numerical simulations, data analysis and drafted the manuscript. FN supervised all the experimental works and formalized the manuscript content. FH, as an expert in the field provided guidance throughout the numerical simulations. MS and AN contributed in the technical content and approved the final version of the manuscript. All authors read and approved the final manuscript.

#### Authors' information

Sani Bida is a lecturer at Federal Polytechnic Bida, Nigeria. Farah N.A. Abdul Aziz and Farzad Hejazi are Associate Professors at the Universiti Putra Malaysia and researchers at Housing Research Centre. Mohd Saleh Jaafar is a Professor and Nabilah Abu Bakar is a Senior Lecturer at the Universiti Putra Malaysia and both are researchers at Housing Research Centre.

#### Funding

The authors would like to acknowledge the fund provider for making this research a reality by paying for all the materials, fabrication and experimental tests through research Grant 06-01-04-SF2364, Ministry of Science and Technology Malaysia (MOSTI).

#### Availability of data and materials

The data sets used in this study would be made available on reasonable request.

#### Declaration

#### Competing interests

The authors declare that they have no competing interests in respect of this paper.

#### Author details

<sup>1</sup>Housing Research Centre (HRC), Department of Civil Engineering, Universiti Putra Malaysia (UPM), 43400 Serdang, Selangor, Malaysia. <sup>2</sup>Department of Civil Engineering, Federal Polytechnic Bida, PMB 55, Bida, Niger State, Nigeria.

Received: 22 November 2020 Accepted: 4 September 2021  
Published online: 06 October 2021

#### References

- Ahmad, A., Maslehuudin, M., & Al-Hadhrami, L. M. (2014). In situ measurement of thermal transmittance and thermal resistance of hollow reinforced precast concrete walls. *Energy and Buildings*, 84, 132–141.
- Al-Abidi, A. A., Mat, S. B., Sopian, K., Sulaiman, M., & Mohammed, A. T. (2013). CFD applications for latent heat thermal energy storage: A review. *Renewable and Sustainable Energy Reviews*, 20, 353–363.
- Al-Ajlan, S. A. (2006). Measurements of thermal properties of insulation materials by using transient plane source technique. *Applied Thermal Engineering*, 26(17–18), 2184–2191.
- Amran, Y. M., Farzadnia, N., & Ali, A. A. (2015). Properties and applications of foamed concrete; a review. *Construction and Building Materials*, 101, 990–1005.
- Amran, Y. M., Rashid, R. S., Hejazi, F., Ali, A. A., Safiee, N. A., & Bida, S. M. (2018). Structural performance of precast foamed concrete sandwich panel subjected to axial load. *KSCCE Journal of Civil Engineering*, 22(4), 1179–1192.
- ASHRAE Handbook. 2009. ASHRAE Handbook-Fundamental: SI Editions, American society of heating, refrigerating and air-conditioning engineers. Inc.: Atlanta, GA, USA. ISBN 9781933742557.
- ASTM C1363-19. 2019. Subcommittee C16.30, Standard test method for thermal performance of building materials and envelope assemblies by means of a hot box apparatus, DOI: <https://doi.org/10.1520/C1363-19>
- Bai, F., & Davidson, J. S. (2015). Analysis of partially composite foam insulated concrete sandwich structures. *Engineering Structures*, 91, 197–209.
- Benayoune, A., Samad, A. A., Trikha, D., Ali, A. A., & Ellinna, S. (2008). Flexural behaviour of pre-cast concrete sandwich composite panel—experimental and theoretical investigations. *Construction and Building Materials*, 22(4), 580–592.
- Boafo, F., Kim, J.-H., & Kim, J.-T. (2016). Performance of modular prefabricated architecture: Case study-based review and future pathways. *Sustainability*, 8(6), 558.
- BS EN 206-1:2000. 2001. British Standards, European Standard: Concrete—Part. 1: Specification, performance, production and conformity.
- Bush, T. D., & Stine, G. L. (1994). Flexural behavior of composite precast concrete sandwich panels with continuous truss connectors. *PCI Journal*, 39(2), 112–121.
- Bush, T. D., Jr., & Wu, Z. (1998). Flexural analysis of prestressed concrete sandwich panels with truss connectors. *PCI Journal*, 43(5), 76.
- Carbonari, G., Cavalaro, S., Cansario, M., & Aguado, A. (2013). Experimental and analytical study about the compressive behavior of eps sandwich panels. *Materiales De Construcción*, 63(311), 393–402.
- Choi, K.-B., Choi, W.-C., Feo, L., Jang, S.-J., & Yun, H.-D. (2015). In-plane shear behavior of insulated precast concrete sandwich panels reinforced with corrugated GFRP shear connectors. *Composites Part B: Engineering*, 79, 419–429.
- Chua, S. C., & Oh, T. H. (2011). Green progress and prospect in Malaysia. *Renewable and Sustainable Energy Reviews*, 15(6), 2850–2861.
- Einea, A., Salmon, D., Fogarasi, G., Culp, T., & Tadros, M. (1991). State-of-the-art of precast sandwich panel system. *PCI Journal*, 36(6), 90–101.
- Frazão, C., Barros, J., Toledo Filho, R., Ferreira, S., & Gonçalves, D. (2018). Development of sandwich panels combining sisal fiber-cement composites and fiber-reinforced lightweight Concrete. *Cement and Concrete Composites*, 86, 206–223.
- Gerlich, V., Sulovská, K., & Zálešák, M. (2013). COMSOL Multiphysics validation as simulation software for heat transfer calculation in buildings: Building simulation software validation. *Measurement*, 46(6), 2003–2012.
- Gervásio, H., Santos, P., da Silva, L. S., & Lopes, A. (2010). Influence of thermal insulation on the energy balance for cold-formed buildings. *Advanced Steel Construction*, 6(2), 742–766. <https://doi.org/10.18057/IAASC.2010.6.2.5>
- Graziani, L., Quagliarini, E., D'Orazio, M., Lenci, S., & Scalbi, A. (2017). A more sustainable way for producing RC sandwich panels on-site and in developing countries. *Sustainability*, 9(3), 472.
- Hacker, J. N., De Saullés, T. P., Minson, A. J., & Holmes, M. J. (2008). Embodied and operational carbon dioxide emissions from housing: A case study on the effects of thermal mass and climate change. *Energy and Buildings*, 40(3), 375–384.
- Hamed, E. (2016). Modeling, analysis, and behavior of load-carrying precast concrete sandwich panels. *Journal of Structural Engineering*, 142(7), 04016036.

- Hamed, E. (2017). Load-carrying capacity of composite precast concrete sandwich panels with diagonal fiber-reinforced-polymer bar connectors. *PCI Journal*, 62(4), 34–44. <https://doi.org/10.15554/pci62.4-03>
- Hodicky, K., Sopal, G., Rizkalla, S., Hulin, T., & Stang, H. (2014). Experimental and numerical investigation of the FRP shear mechanism for concrete sandwich panels. *Journal of Composites for Construction*, 19(5), 04014083.
- Joseph, J. D. R., Prabakar, J., & Alagusundaramoorthy, P. (2017). Precast concrete sandwich one-way slabs under flexural loading. *Engineering Structures*, 138, 447–457.
- Kim, J., & You, Y.-C. (2015). Composite behavior of a novel insulated concrete sandwich wall panel reinforced with GFRP shear grids: Effects of insulation types. *Materials*, 8(3), 899–913.
- Lee, B.-J., & Pessiki, S. (2006). Thermal behavior of precast prestressed concrete three-wythe sandwich wall panels, Architectural Engineering Conference (AEI) 2006: Building Integration Solutions (pp. 1–15).
- Lee, B.-J., & Pessiki, S. (2008). Experimental evaluation of precast, prestressed concrete, three-wythe sandwich wall panels. *PCI Journal*, 53(2), 95–115.
- Menoufi, K., Castell, A., Navarro, L., Pérez, G., Boer, D., & Cabeza, L. F. (2012). Evaluation of the environmental impact of experimental cubicles using Life Cycle Assessment: A highlight on the manufacturing phase. *Applied Energy*, 92, 534–544.
- Mohamad, N., & Muhammad, H. M. (2011). *Testing of precast lightweight foamed concrete sandwich panel with single and double symmetrical shear truss connectors under eccentric loading*. Advanced Materials Research (Volumes 250–253) Edited by Guangfan Li, Yong Huang and Chaohe Chen, <https://doi.org/10.4028/www.scientific.net/AMR.335-336.1107>
- Mohamad, N., Omar, W., & Abdullah, R. (2011). *Precast Lightweight Foamed Concrete Sandwich Panel (PLFP) tested under axial load: preliminary results*. Advanced Materials Research (Volumes 250–253) Edited by Guangfan Li, Yong Huang and Chaohe Chen, 1153–1162, <https://doi.org/10.4028/www.scientific.net/AMR.250-253.1153>. Paper presented at the Advanced Materials Research.
- Mohamad, N., & Hassan, N. (2013). *The structural performance of precast lightweight foam concrete sandwich panel with single and double shear truss connectors subjected to axial load*. Paper presented at the Advanced Materials Research. <https://doi.org/10.4028/www.scientific.net/AMR.634-638.2746>
- Naito, C., Hoemann, J., Beacraft, M., & Bewick, B. (2011). Performance and characterization of shear ties for use in insulated precast concrete sandwich wall panels. *Journal of Structural Engineering*, 138(1), 52–61.
- Pérez-Lombard, L., Ortiz, J., & Pout, C. (2008). A review on buildings energy consumption information. *Energy and Buildings*, 40(3), 394–398.
- Retzlaff, R. C. (2009). Green buildings and building assessment systems: A new area of interest for planners. *Journal of Planning Literature*, 24(1), 3–21.
- Royon, L., Karim, L., & Bontemps, A. (2013). Thermal energy storage and release of a new component with PCM for integration in floors for thermal management of buildings. *Energy and Buildings*, 63, 29–35.
- Salmon, D. C., Einea, A., Tadros, M. K., & Culp, T. D. (1997). Full scale testing of precast concrete sandwich panels. *ACI Structural Journal*, 94, 239–247. <https://doi.org/10.14359/486>
- Sartori, I., Napolitano, A., & Voss, K. (2012). Net zero energy buildings: A consistent definition framework. *Energy and Buildings*, 48, 220–232.
- Teixeira, N., Tomlinson, D. G., & Fam, A. (2016). Precast concrete sandwich wall panels with bolted angle connections tested in flexure under simulated wind pressure and suction. *PCI Journal*. <https://doi.org/10.15554/pci61.4-02>
- Tomlinson, D., & Fam, A. (2014). Experimental investigation of precast concrete insulated sandwich panels with glass fiber-reinforced polymer shear connectors. *ACI Structural Journal*, 111(3), 595.
- Tomlinson, D., & Fam, A. (2016). Analytical approach to flexural response of partially composite insulated concrete sandwich walls used for cladding. *Engineering Structures*, 122, 251–266.
- Van Schijndel, A., Schellen, H., & De Wit, M. (2009). Improved HVAC operation to preserve a church organ. *Building and Environment*, 44(1), 156–168.
- Woltman, G., Noel, M., & Fam, A. (2017). Experimental and numerical investigations of thermal properties of insulated concrete sandwich panels with fiberglass shear connectors. *Energy and Buildings*, 145, 22–31.
- Zhi, Q., & Guo, Z. (2017). Experimental evaluation of precast concrete sandwich wall panels with steel-glass fiber-reinforced polymer shear connectors. *Advances in Structural Engineering*, 20(10), 1476–1492.

## Publisher's Note

Springer Nature remains neutral with regard to jurisdictional claims in published maps and institutional affiliations.

Submit your manuscript to a SpringerOpen® journal and benefit from:

- Convenient online submission
- Rigorous peer review
- Open access: articles freely available online
- High visibility within the field
- Retaining the copyright to your article

Submit your next manuscript at ► [springeropen.com](https://www.springeropen.com)